



Temperate and chronic virus competition leads to low lysogen frequency

Sara M. Clifton^{a,*}, Rachel J. Whitaker^{b,c}, Zoi Rapti^{c,d}



^a Department of Mathematics, Statistics, and Computer Science, St. Olaf College, Northfield, MN 55057, USA

^b Department of Microbiology, University of Illinois at Urbana-Champaign, Urbana, IL 61801, USA

^c Carl R. Woese Institute for Genomic Biology, University of Illinois at Urbana-Champaign, Urbana, IL 61801, USA

^d Department of Mathematics, University of Illinois at Urbana-Champaign, Urbana, IL 61801, USA

ARTICLE INFO

Article history:

Received 17 November 2019

Revised 4 April 2021

Accepted 5 April 2021

Available online 9 April 2021

Keywords:

Bacteria

Phage

Latent

Infection

Recovery

Mathematical model

ABSTRACT

The canonical bacteriophage is obligately lytic: the virus infects a bacterium and hijacks cell functions to produce large numbers of new viruses which burst from the cell. These viruses are well-studied, but there exist a wide range of coexisting virus lifestyles that are less understood. Temperate viruses exhibit both a lytic cycle and a latent (lysogenic) cycle, in which viral genomes are integrated into the bacterial host. Meanwhile, chronic (persistent) viruses use cell functions to produce more viruses without killing the cell; chronic viruses may also exhibit a latent stage in addition to the productive stage. Here, we study the ecology of these competing viral strategies. We demonstrate the conditions under which each strategy is dominant, which aids in control of human bacterial infections using viruses. We find that low lysogen frequencies provide competitive advantages for both virus types; however, chronic viruses maximize steady state density by eliminating lysogeny entirely, while temperate viruses exhibit a non-zero 'sweet spot' lysogen frequency. Viral steady state density maximization leads to coexistence of temperate and chronic viruses, explaining the presence of multiple viral strategies in natural environments.

© 2021 Elsevier Ltd. All rights reserved.

1. Introduction

All viruses depend upon their hosts for reproduction. Viruses have evolved many strategies to reproduce within bacteria, including the lytic, temperate, and chronic lifestyles within the bacterial host (Calendar, 2006; Dimmock et al., 2016; Weinbauer, 2004). After infection, lytic viruses replicate within the bacterial host and transmit by bursting from the cell, killing the host. Temperate viruses have both a lytic cycle and a latent cycle, in which the viral genetic material is integrated into host genomes; latent viruses remain dormant in the bacterial genome until induced to replicate (Weinbauer, 2004). In chronic infection, productive host cells bud new viruses from the cell without killing the bacterium (Rakonjac, 2012). Chronic viruses may also have a latent cycle in which viral genetic material is incorporated into the bacterium's genome, and the cell transmits the virus's genetic material (provirus) to daughter cells vertically (Lwoff, 1953). Comparative genomics among closely related bacterial strains has uncovered a plethora of proviruses of both temperate and chronic lifestyles (Davies et al., 2016; Roux et al., 2015; Mathee et al., 2008;

Mosquera-Rendón et al., 2016; Spencer et al., 2003; Kung et al., 2010).

Viruses of all four lifestyle classes infect many bacteria relevant to human disease treatment, especially immunocompromised patients vulnerable to common bacterial infections. In particular, patients with cystic fibrosis or serious burns may become infected with the ubiquitous *Pseudomonas aeruginosa*, which can lead to patient death within days if unsuccessfully treated (Courtney et al., 2007; Emerson et al., 2002; Nixon et al., 2001). Because *P. aeruginosa* is often resistant to multiple antibiotic treatments (Jarvis and Martone, 1992; Hancock and Speert, 2000; US Department of Health and Human Services, 2013), phage therapy (Altamirano and Barr, 2019; Sulakvelidze et al., 2001) and phage-antibiotic synergistic (PAS) therapy (Lin et al., 2018; Comeau et al., 2007; Kutter et al., 2010) are now being studied to treat bacterial infections. Response to these treatments depends significantly on the ecology of the bacteria-virus system already present within the human host (Clifton et al., 2019); therefore it is critical to understand the environmental and evolutionary conditions under which each viral strategy is dominant in order to provide effective treatment.

While mathematical models of lytic viruses (e.g., Weitz and Dushoff, 2008; Payne and Jansen, 2001) and temperate viruses (e.g., Sinha et al., 2017) have been studied extensively, relatively few models of chronic viruses (e.g., Gulbudak and Weitz, 2019;

* Corresponding author.

E-mail address: clifto2@stolaf.edu (S.M. Clifton).

Weitz et al., 2019; Clifton et al., 2019) have been examined. To our knowledge, no studies have rigorously analyzed the ecological interactions among bacteria and all four viral lifestyles: lytic, latent lytic, chronic, and latent chronic. Several important open questions exist that neither experimental nor modeling efforts have yet answered in this context:

1. Experiments have found that temperate virus lysogen frequencies tend to be small ($\sim 1\%$ of infections) (Calendar, 2006). What are the theoretical underpinnings of this phenomenon?
2. Lysogen frequencies for temperate viruses have been well-studied both experimentally and theoretically (Calendar, 2006; Oppenheim and Adhya, 2007; Volkova et al., 2014), but lysogen frequencies for chronic viruses have not been determined. What is the predicted range of lysogen frequencies for chronic viruses?
3. Bacterial recovery (cure) rates from viral infection have not been quantified either experimentally or theoretically. Most mathematical models ignore recovery for simplicity (e.g., Weitz et al., 2019). Experimentally, a wide range of recovery rates has been observed; some proviruses remain viable over evolutionary timescales (implying recovery rates near zero) (Brüssow et al., 2004), and some proviruses are inactivated nearly instantly by CRISPR systems (implying extremely fast recovery rates) (Horvath and Barrangou, 2010). Can we establish a narrower range of typical recovery rates?

In this paper we develop a mathematical model of the competition between temperate and chronic viruses for bacterial hosts, using *P. aeruginosa* infections within humans as a case study. An analysis of this model yields simple and intuitive answers to the preceding questions.

2. Model

With the goal of understanding competition between two viral strategies, temperate viruses V_T with lytic and latent stages and chronic viruses V_C with productive and latent chronic stages, we develop a simple model of the bacteria-virus ecosystem (see Fig. 1 for the model overview). Each virus may infect a single strain of bacteria that is initially susceptible (S) to both viral types. We assume the total bacterial population grows logistically to a carrying capacity K (Zwietering et al., 1990). All bacteria population densities are rescaled to be proportions of the carrying capacity. Susceptible bacteria grow at an intrinsic rate r_S , and infected bacteria may grow at either faster or slower rates (Shapiro et al., 2016). In the model system, the timescale is rescaled such that all rates are relative to r_S .

Temperate viruses infect susceptible bacteria at a rate η_T ; the infected bacteria will either become latently infected L_T with probability f_T , or will enter a lytic state I_T with probability $1 - f_T$. Bacteria in the lytic state produce viruses and burst (with burst size β_T) at a rate δ . While in the lytic state, the virus hijacks cell functions, and the cell cannot reproduce (Tabib-Salazar et al., 2017; St-Pierre and Endy, 2008). Bacteria in the latent lytic state reproduce at a rate r_T . Bacteria do not move between lytic and latent states unless the system is stressed (e.g., by heat or sublethal antibiotics); we ignore spontaneous induction because it is a rare occurrence (Nanda et al., 2015; Garro and Law, 1974; Cortes et al., 2019). However, lytic and latent lytic bacteria may recover from infection at rates γ_I and γ_T , respectively (Casjens, 2003; Brüssow et al., 2004).

Similarly, chronic viruses infect susceptible bacteria at a rate η_C , leading to either latent infection L_C with probability f_C or productive infection P_C with probability $1 - f_C$ (Hobbs and Abedon, 2016).

Bacteria in the productive state reproduce at a rate r_P and produce viruses at a rate β_C without cell death. While in the latent chronic state, bacteria reproduce at a rate r_C . Unless the system is stressed, bacteria will not switch from latent to productive states, but productive and latent chronic bacteria may recover at rate γ_P and γ_C , respectively (Casjens, 2003; Brüssow et al., 2004). Again, we ignore spontaneous induction due to its rarity (Nanda et al., 2015; Garro and Law, 1974; Cortes et al., 2019).

Once a bacterium is infected, we assume it will exclude both superinfection by the same viral type and cross infection by viruses of the other type (De Smet et al., 2017). Outside the cell, free temperate viruses and free chronic viruses decay naturally at rates μ_T and μ_C , respectively (Heldal and Bratbak, 1991).

The following Eqs. (1)–(7) are the dynamical systems model that captures the preceding qualitative description. See Table 1 for variable descriptions, Table 2 for parameter descriptions and relevant values, and Appendix D for the model rescaling.

$$\dot{S} = \underbrace{S(1-N)}_{\text{growth}} - \underbrace{\eta_T SV_T - \eta_C SV_C}_{\text{infection}} + \underbrace{\gamma_T L_T + \gamma_I I_T + \gamma_P P_C + \gamma_C L_C}_{\text{recovery}} \quad (1)$$

$$\dot{I}_T = \underbrace{\eta_T(1-f_T)SV_T}_{\text{infection}} - \underbrace{\delta I_T}_{\text{lysis}} - \underbrace{\gamma_I I_T}_{\text{recovery}} \quad (2)$$

$$\dot{L}_T = \underbrace{r_T L_T(1-N)}_{\text{growth}} + \underbrace{\eta_T f_T SV_T}_{\text{infection}} - \underbrace{\gamma_T L_T}_{\text{recovery}} \quad (3)$$

$$\dot{P}_C = \underbrace{r_P P_C(1-N)}_{\text{growth}} + \underbrace{(1-f_C)\eta_C SV_C}_{\text{infection}} - \underbrace{\gamma_P P_C}_{\text{recovery}} \quad (4)$$

$$\dot{L}_C = \underbrace{r_C L_C(1-N)}_{\text{growth}} + \underbrace{f_C \eta_C SV_C}_{\text{infection}} - \underbrace{\gamma_C L_C}_{\text{recovery}} \quad (5)$$

$$\dot{V}_T = \underbrace{\beta_T \delta I_T}_{\text{burst}} - \underbrace{\eta_T SV_T}_{\text{adsorption}} - \underbrace{\mu_T V_T}_{\text{degradation}} \quad (6)$$

$$\dot{V}_C = \underbrace{\beta_C P_C}_{\text{production}} - \underbrace{\eta_C SV_C}_{\text{adsorption}} - \underbrace{\mu_C V_C}_{\text{degradation}} \quad (7)$$

Note that infection rates for temperate and chronic viruses, although assumed constant, may depend on the bacterial population; many relevant bacteria form biofilms at high density that protect the population from infection (Harper et al., 2014). For simplicity, we have also assumed that lysogen frequencies are constant, but some studies have demonstrated that bacterial density may impact lysogeny rates (Hargreaves et al., 2014; Silpe and Bassler, 2018). These simplifications are necessary for analytic tractability.

3. Results

Although this model is applicable to any bacteria-virus ecosystem with both temperate and chronic viral lifestyles, we present model predictions using parameters taken from the human pathogens *P. aeruginosa* or *E. coli* and their viruses (see Table 2). Besides their medical relevance, *P. aeruginosa* and *E. coli* are among the most well-studied microbes in science. We initialize the system with $S(0) = 1e-3$, $V_T(0) = V_C(0) = 1e-7$ and all others zero, following Sinha et al. (2017); no bistability exists for our parameter values, so the initial condition does not affect the steady state (see Appendix C). Because we are primarily interested in recovery from infection that is passed vertically to daughter cells, we take $\gamma_I = 0$ for the remainder of the paper. The results are qualitatively similar for $\gamma_I > 0$; see Appendix for full model analysis.

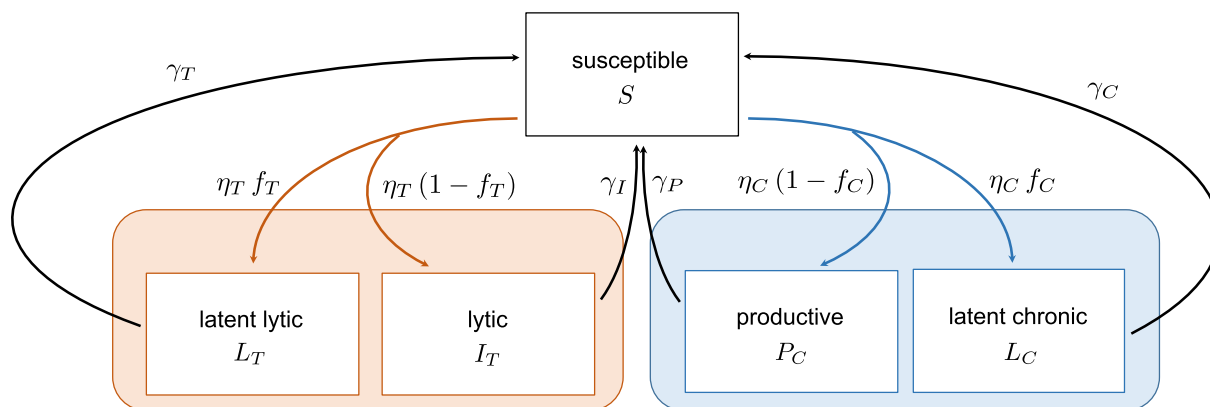


Fig. 1. Flowchart of model Eqs. (1)–(7). Arrows indicate infection by temperate viruses (orange), infection by chronic viruses (blue), or recovery from infection (black). Infection rates are denoted η_i , recovery (cure) rates are denoted γ_i , and lysogen frequencies are denoted f_i .

Table 1

Description of model variables in bacteria-virus system (1)–(7). All densities are scaled by the bacterial carrying capacity^a and time is scaled by the growth rate of uninfected bacteria^b. See Appendix D for the model rescaling process.

Variable	Meaning	Units
S	susceptible bacteria as a proportion of carrying capacity	unitless
I_T	lytic bacteria as a proportion of carrying capacity	unitless
L_T	latent lytic bacteria as a proportion of carrying capacity	unitless
P_C	productive bacteria as a proportion of carrying capacity	unitless
L_C	latent chronic bacteria as a proportion of carrying capacity	unitless
N	all bacteria ($S + I_T + L_T + P_C + L_C$)	unitless
V_T	ratio of free temperate viruses to bacteria carrying capacity	$\frac{\text{PFU}}{\text{CFU}}$
V_C	ratio of free chronic viruses to bacteria carrying capacity	$\frac{\text{PFU}}{\text{CFU}}$
t	time rescaled by intrinsic growth rate	unitless

^a Stable bacterial density in human hosts is highly variable; a study of viable *P. aeruginosa* densities in sputum of 12 patients with cystic fibrosis not undergoing treatment ranged from 5.3e3 CFU/mL to 1.8e11 CFU/mL (Stressmann et al., 2011; Price et al., 2013).

^b Growth rate is approximately $5.1 \times 10^{-3} \text{ min}^{-1}$ for *P. aeruginosa* grown *in vitro*, but is highly variable in human hosts (Spalding et al., 2018; Kopf et al., 2016).

3.1. Model behavior

In Fig. 2, we simulate the model system for the baseline parameter values in Table 2. We see a rapid initial growth of the susceptible population followed quickly by a population crash caused primarily by lytic infection (see Fig. 3(a)). Filling the niche created by the susceptible population crash are the latent lytic bacteria. As the latent lytic, lytic, and susceptible populations settle at nearly steady levels, the productive bacterial population grows exponentially (see Fig. 3(b)). After dozens of bacterial divisions, the productive bacteria overtake the latent lytic bacteria, and the latent lytic bacterial population quickly declines. At steady state, the productive bacteria are the most abundant in the system because chronic viruses do not require new susceptible bacteria in order to reproduce.

Although chronically infected bacteria dominate the system, free temperate viruses stabilize at over twice the density of free chronic viruses (Fig. 2b). Although little is known about the proportion of each viral type seen in natural environments, it is known that temperate and chronic viruses frequently coexist Winstanley et al., 2009. The model predicts that the total virus to total bacteria ratio stabilizes at 58:1, which falls within the typical range of virus

¹ Total free-phage density exceeded that of *P. aeruginosa* by a factor of 11-fold to 90-fold in sputum samples from patients with cystic fibrosis.

to bacteria ratios seen in natural environments¹ (James et al., 2015; Knowles et al., 2016).

The model behaviors presented here use the baselines in Table 2. However, the equilibria and their respective stability depends on nearly all the model parameters (see the Appendix for more details).

3.2. Steady states and stability

While many evolvable parameters (such as viral burst sizes and bacterial growth rates) are likely limited by physical constraints, lysogen frequency could theoretically take on any value. Lysogen frequency is of particular interest because latency involves inherent tradeoffs between vertical and horizontal transmission; the lytic strategy relies on horizontal transmission only, while the latent strategy uses only vertical transmission.

Therefore, our primary interest for this study is the lysogen frequencies for temperate and chronic viruses; we look at the possible steady state outcomes for all possible combinations of lysogen frequencies f_T and f_C with all other parameters held constant at the baselines in Table 2. Only four stable steady states exist: **coexistence** (all populations exceed 0), **temperate strategy only** ($V_C = P_C = L_C = 0$), **chronic strategy only** ($V_T = I_T = L_T = 0$), and **susceptible only** (all populations, except S , are 0). See Fig. 4 for the bifurcation diagram.

Temperate viruses can outcompete chronic viruses if the temperate lysogen frequency is neither too large nor too small (see ‘Temperate only’ region of Fig. 4). If the temperate lysogen frequency is too high, then chronic viruses will be produced in large numbers relative to temperate; chronic viruses will infect susceptible bacteria first, eventually driving temperate viruses to extinction (see ‘Chronic only’ region of Fig. 4). If the temperate lysogen frequency is too low, then temperate viruses lyse bacteria too quickly, leaving room for productive bacteria to reproduce while the susceptible population also grows; if the productive bacterial population is large enough (i.e., chronic lysogen frequencies are sufficiently low), then both viral types will coexist (see ‘Coexistence’ region of Fig. 4). See Appendices A and C for the complete steady state analysis.

3.3. Temperate viruses exhibit a ‘sweet spot’ lysogen frequency

Temperate viruses are known to exhibit a small, nonzero lysogen frequency (Calendar, 2006; Oppenheim and Adhya, 2007; Volkova et al., 2014; Yu et al., 2017; El Didamony et al., 2015; Latino et al., 2014; Schrader et al., 1997; Ceysens et al., 2010; Garbe et al., 2011; You et al., 2002). Our model illustrates why tem-

Table 2

Description of model parameters in bacteria-virus system (1)–(7). See Appendix D for the model rescaling process and Appendix E for the parameter selection process.

Parameter	Meaning	Range ^a	Baseline	Sources
r_T, r_P, r_C	growth rates of (respectively) latent lytic, productive, and latent chronic bacteria relative to the susceptible bacteria growth rate ^b	[0.5, 3] ^c	1	Shapiro et al. (2016)
η_T, η_C	infection rate of (respectively) temperate and chronic viruses	[0.38, 14.7] ^d	1	Sinha et al. (2017)
$\gamma_T, \gamma_P, \gamma_C$	recovery rates of (respectively) latent lytic, productive, and latent chronic bacteria	[0, 1000] ^e	0.67 ^f	Brüssow et al. (2004) and Horvath and Barrangou (2010)
γ_l	recovery rates of lytic bacteria	[0, 1000]	0 ^g	Brüssow et al. (2004) and Horvath and Barrangou (2010)
δ	rate at which lytic infection leads to bursting (eclipse and rise phase)	[1.5, 7.8] ^h	4	Yu et al. (2017) and El Didamony et al. (2015)
f_T	lysogen frequency for temperate viruses	[0, 0.9]	0.01	Calendar (2006), Oppenheim and Adhya (2007) and Volkova et al. (2014)
f_C	lysogen frequency for chronic viruses	[0, 0.9]	0 ^f	Calendar (2006), Oppenheim and Adhya (2007) and Volkova et al. (2014)
β_T	burst size for bacteria infected with V_T	[10, 1000]	100	Yu et al. (2017), El Didamony et al. (2015), Latino et al. (2014), Schrader et al. (1997), Ceyskens et al. (2010), Garbe et al. (2011) and You et al. (2002)
β_C	viral production rate for bacteria infected with V_C	[5, 200]	20	Clifton et al. (2019)
μ_T, μ_C	degradation rate of (respectively) free temperate viruses and free chronic viruses	[0.9, 3.6] ⁱ	1	Heldal and Bratbak (1991)

^a All parameter ranges are taken for the human pathogens *P. aeruginosa* or *E. coli* and their viruses, unless otherwise noted.^b Growth rate is approximately $5.1 \times 10^{-3} \text{ min}^{-1}$ for *P. aeruginosa* grown *in vitro*, but is highly variable in human hosts.^c Estimates based on *E. coli* and M13 phage.^d Estimates based on *E. coli* and λ phage.^e A wide range of recovery rates has been found; some proviruses are viable over evolutionary timescales and some proviruses are inactivated nearly instantly by CRISPR systems.^f Estimated from viral steady state density (see Results section).^g Selected to be 0 to simplify model analysis; allowing $\gamma_l = \gamma_T$ produces qualitatively similar results, so the increased model complexity is not justified.^h Low estimate is for PAXYB1 phage and PAO1 host, high estimate is for ϕ PSZ1 phage and PAO1 host.ⁱ Low estimate is for viruses extracted from Raunefjorden, high estimate is for viruses extracted from Bergen Harbor (strains unknown).

perate viruses have a theoretical ‘sweet spot’ lysogen frequency when competing with chronic viruses.

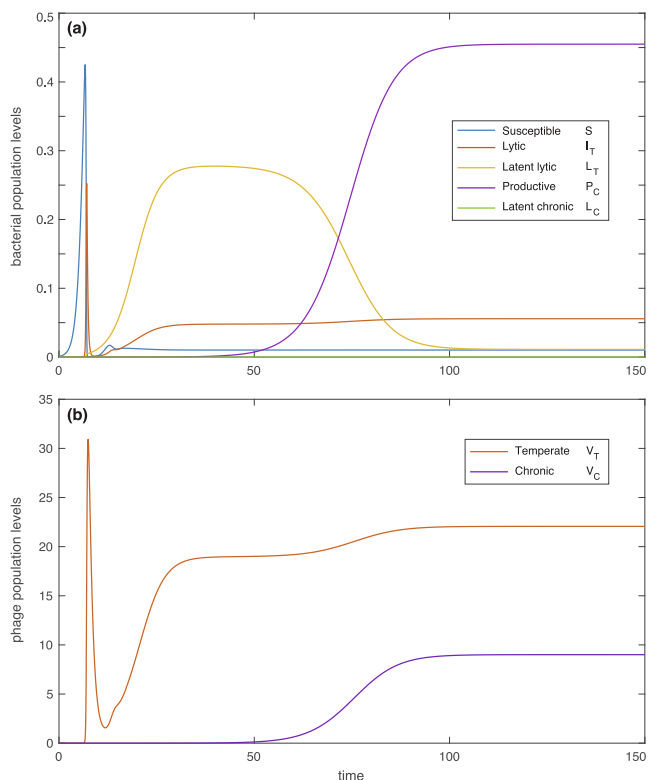


Fig. 2. Simulation of model Eqs. (1)–(7). Initial conditions are $S(0) = 1e - 3, V_T(0) = V_C(0) = 1e - 7$ with all others zero. All parameters are held constant at the baseline values given in Table 2. Eventually the temperate and chronic viral strategies reach a stable coexistence state.

Suppose that temperate viruses select² a lysogen frequency f_T that maximizes steady state viral abundance, including both free viruses (V_T) and proviruses (L_T , as proxy). Because chronic viruses may also select a lysogen frequency f_C that maximizes their viral density, the optimal lysogen frequency for temperate viruses depends on f_C .

Fig. 5(a) shows the steady state temperate viral density for all possible combinations of f_T and f_C . Given any chronic lysogen frequency f_C , temperate viruses may select a lysogen frequency f_T that conditionally maximizes their viral density (optimal strategies are shown in red). We see that for all possible chronic latency strategies, there exists a small but nonzero (i.e., sweet spot) lysogen frequency f_T that maximizes temperate viral density at steady state.

3.4. Chronic viruses should eliminate latency

While lysogen frequencies for temperate viruses are well-studied, lysogen frequencies for chronic viruses are unknown. Our model reveals that the lysogen frequency for chronic viruses should be exactly zero. In Fig. 5(b), we plot the steady state density of chronic viruses in the system ($V_C + L_C$). For any given temperate viral lysogen frequency f_T , chronic viruses maximize steady state density by selecting a lysogen frequency $f_C = 0$. From an ecological perspective, this result is intuitive. We have assumed that there is no reproductive cost to productive infection relative to latent infection, so it benefits chronic viruses to spread genetic material both horizontally (via production) and vertically (via cell division), rather than vertically alone.

3.5. Bacterial recovery rate determinable using viral abundance

We use our conclusion that $f_C = 0$, along with the fact that temperate viruses possess a lysogen frequency around 1% to deduce

² We use ‘select’ in the sense of evolutionary game theory.

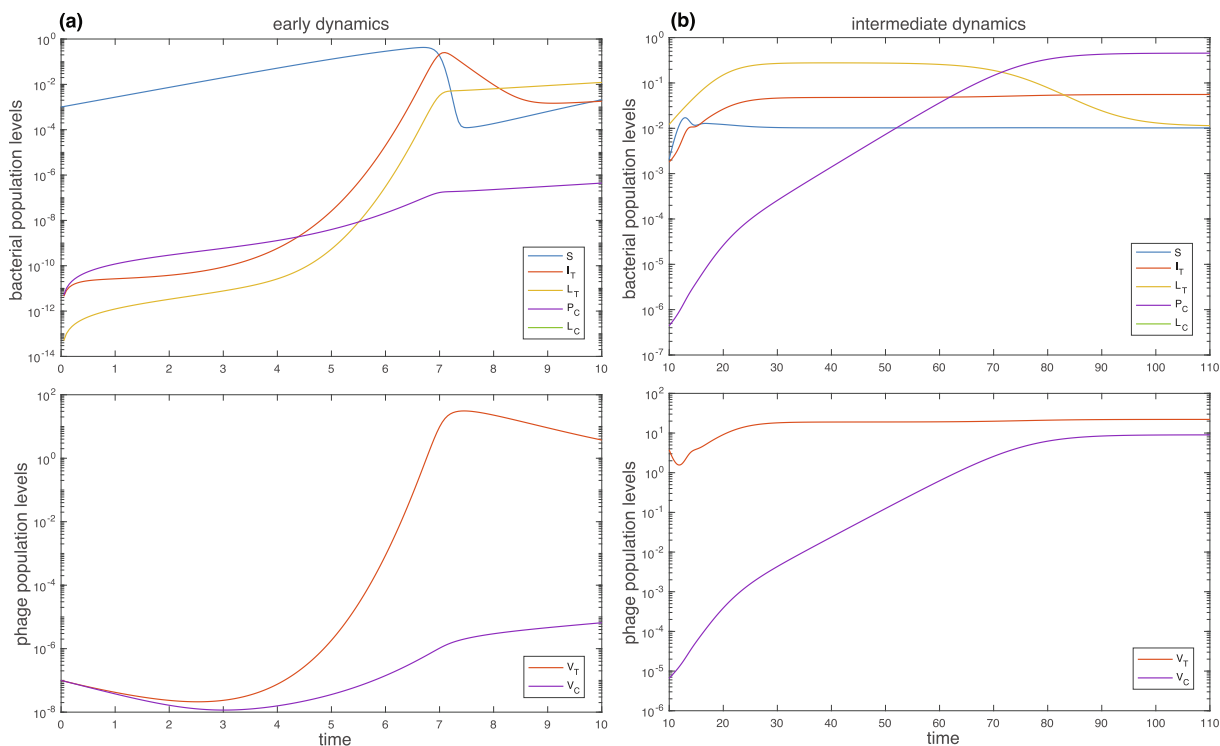


Fig. 3. Transient behavior of Eqs. (1)–(7), plotted on a logarithmic scale. (a) For the first 7–8 bacterial divisions, susceptible bacteria (S) grow exponentially before suddenly crashing. At the same time, temperate infections (I_T, L_T) grow super-exponentially, as do chronic infections (P_C) to a lesser extent. (b) After the early dynamics, the temperate infections approximately stabilize, while the chronic infection grows exponentially. Eventually the chronically infected bacteria overtake the temperately infected bacteria, which crash to a relatively low population level. After about 100 bacterial divisions (about 13.6 days), the temperate and chronic viral strategies reach a stable coexistence state. Note that $L_C(t) = 0$, and therefore does not appear in the figures.

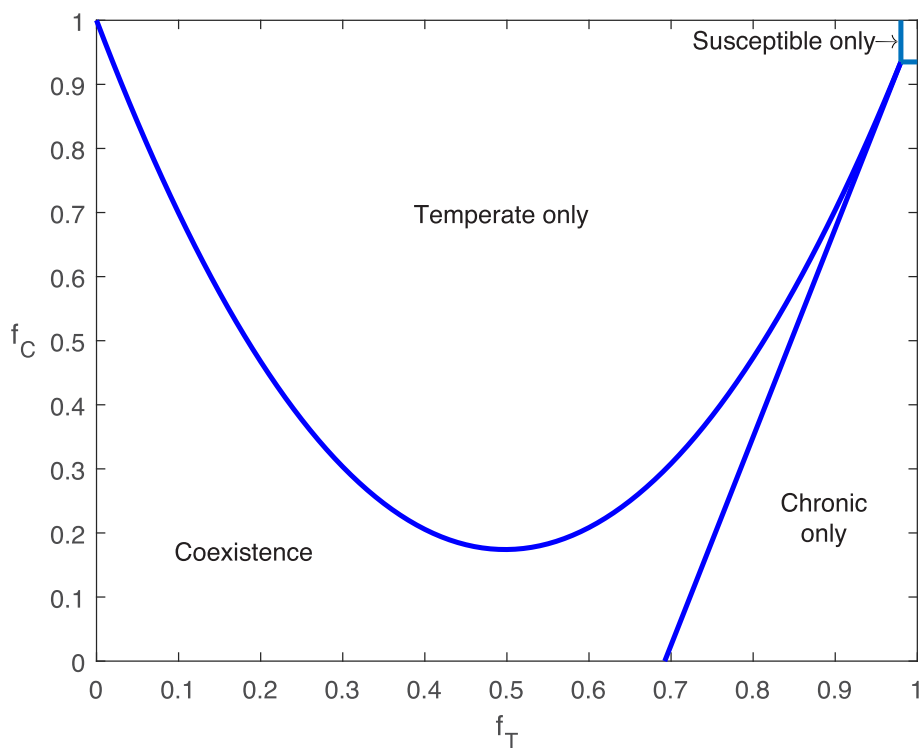


Fig. 4. Bifurcation diagram of lysogen frequencies for temperate and chronic viruses. Holding all other parameters constant at the baseline values given in Table 2, we find that four steady state outcomes are possible: coexistence of both viral strategies, temperate survival with chronic extinction, chronic survival with temperate extinction, and extinction of both viral strategies (susceptible bacteria the only survivors). If the lysogen frequency for a particular viral type is too high, then that virus will not survive. If lysogen frequencies are low enough for both viral types, then the viruses will coexist. This bifurcation diagram was generated using standard linear stability analysis; see Appendix B for details on the viral invasion analysis.

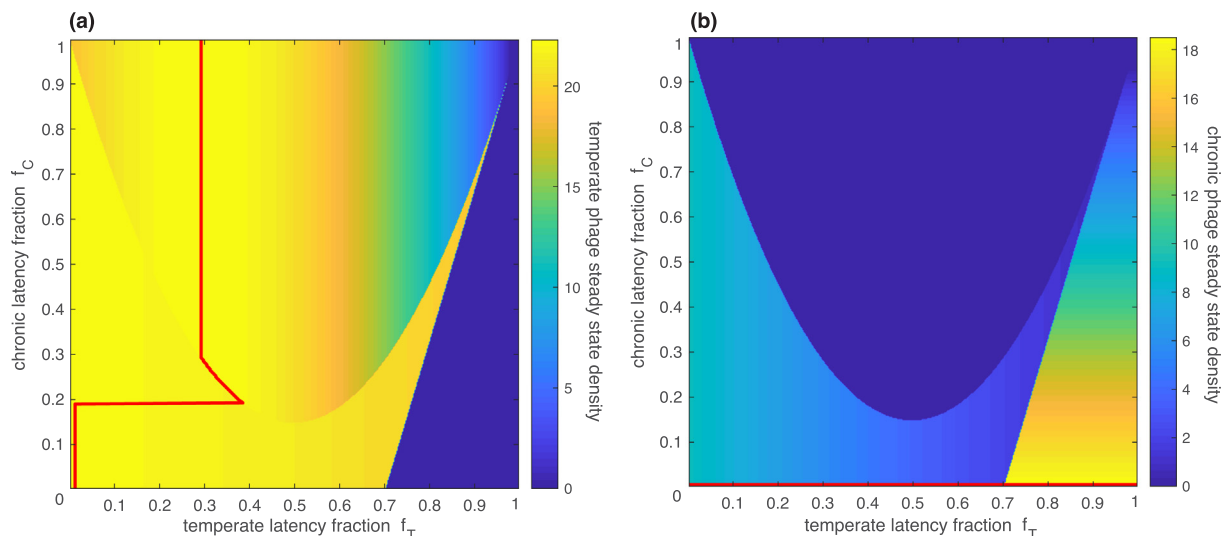


Fig. 5. Viral steady state density over the full range of possible lysogen frequencies ($0 \leq f_i \leq 1$) for temperate and chronic viruses. Color indicates the steady state viral density, and the red line is the maximum steady state density for each lysogen frequency of the competing virus. (a) Temperate virus density ($V_T + L_T$) at steady state. The red curve shows the maximum steady state density for every possible chronic lysogen frequency. Note that the optimal temperate lysogen frequency jumps from nearly 40% lysogeny to about 1% lysogeny when the chronic lysogen frequency drops below 20%. This rapid transition occurs because the optimal state for the temperate virus jumps from a temperate only state to a coexistence steady state. (b) Chronic virus density ($V_C + L_C$) at steady state. The red curve shows that the maximum steady state density for every possible chronic lysogen frequency is $f_C = 0$. Taking these two steady state density profiles together, it is evident that chronic viruses should avoid latency ($f_C = 0$), and therefore temperate viruses should adopt a lysogen frequency near $f_T = 0.01$.

the typical bacterial recovery (cure) rates. In the interest of simplicity, we assume all recovery rates are equal: $\gamma = \gamma_T = \gamma_P = \gamma_C$. The appropriate recovery rates should lead to a maximum temperate virus steady state density ($V_T + L_T$) for $f_C = 0$ and $f_T \approx 0.01$, which occurs over only a small range of $\gamma \approx 0.67$ ($3.4e-3$ per minute); see Fig. 5(a).

A wide range of outcomes is possible if the recovery rate γ is not near 0.67 (see Fig. 6), but none include temperate lysogen frequencies near 1% and coexistence of both viral types, as we see in many natural environments.

For $\gamma \leq 0.2$ (very slow intracellular provirus deactivation), optimal temperate lysogen frequencies are $f_T = 0$ when chronic viruses select the optimal lysogen frequency of $f_C = 0$ (see Fig. 6). However, temperate viruses are effectively driven to extinction under these conditions, implying that extremely stable proviruses are deleterious to temperate viruses. Due to the presence of both viral types in many environments, we suspect that intracellular provirus deactivation is not extremely slow.

For moderately slow intracellular provirus deactivation ($0.22 \leq \gamma \leq 0.66$), optimal temperate lysogen frequencies exceed 5% (see Fig. 6). This result implies that temperate viruses more resilient to deactivation should also increase latency.

If instead $0.68 \leq \gamma \leq 0.79$ (moderately fast intracellular provirus deactivation), then the optimal temperate lysogen frequency is exactly zero again (see Fig. 6). In other words, for faster recovery rates, all temperate viruses would be obligately lytic. Due to this result, we speculate that temperate proviruses are more resilient to intracellular deactivation than obligately lytic viruses.

For $\gamma \geq 0.8$ (very fast intracellular deactivation), lysogen frequencies instantaneously jump to around $f_T = 0.5$, and chronic viruses are driven to extinction (see Fig. 6).

4. Discussion

4.1. Recovery rates and lysogen frequencies

In environments where temperate and chronic viruses coexist, bacterial recovery rates should fall in a fairly narrow range to pro-

duce the observed lysogen frequencies. For the parameter values selected for our study, we find $\gamma = 0.67$ ($3.4e-3$ per minute). If proviruses are slightly more stable, then we would expect to see higher lysogen frequencies for temperate viruses. For proviruses that are stable on evolutionary timescales, we would expect to see chronic viruses dominate. For proviruses that are slightly less stable, we would expect to see the latency strategy disappear. For proviruses that are quickly deactivated, we would expect to see temperate viruses dominate with large lysogen frequencies. Our predicted recovery rate is faster than one might expect, so we hope this study encourages more experimental work on the intracellular deactivation of proviruses within *P. aeruginosa*.

4.2. Limitations

With the goal of keeping the model analytically tractable, we have made simplifying assumptions that may affect the presented results. First, we have assumed mass action infection dynamics, but *P. aeruginosa*-virus infection rates may not be well-approximated by a mass action process, especially for large bacteria population sizes (Simmons et al., 2017; Vidakovic et al., 2018). More realistically, infection rates may slow as population growth activates quorum-sensing and biofilm formation (Harper et al., 2014).

In addition, we have assumed the lytic recovery rate is zero and all other recovery rates are equal. Although assuming $\gamma_l = 0$ produces qualitatively similar results to $\gamma_l = \gamma_T$, it may not be reasonable to assume that all other recovery rates are equal. Future study is needed to determine how recovery rates are affected by the infection type.

We have also assumed that both viral types produce super-infection and cross-infection exclusion proteins that prevent a second infection of any kind. While many viruses that infect *P. aeruginosa* produce super-infection exclusion proteins that effectively prevent multiple infections by the same viral type (Heo et al., 2007; James et al., 2012), little is known about cross resistance to viral infection.

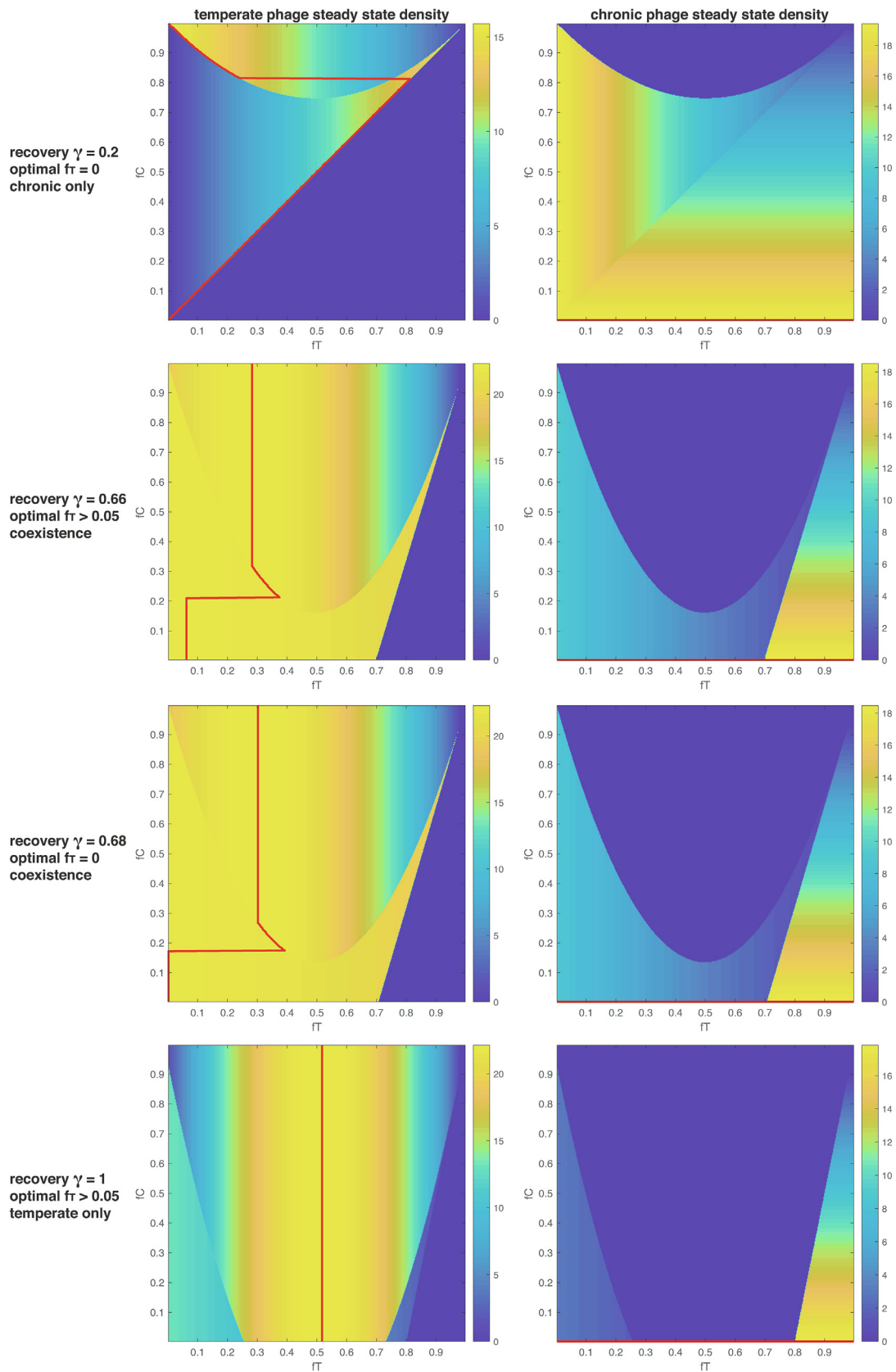


Fig. 6. Viral steady state density over the full range of possible lysogen frequencies ($f_i \in [0, 1]$) for temperate and chronic viruses. Color indicates the steady state viral density, and the red line is the maximum steady state density for each lysogen frequency of the competing virus. Left panel is temperate virus density ($V_T + L_T$) at steady state. Right panel is chronic virus density ($V_C + L_C$) at steady state. Top row is $\gamma = 0.2$, followed by $\gamma = 0.66$, $\gamma = 0.68$, and the bottom row is $\gamma = 1$.

Another simplifying assumption is that lysogen frequencies are constant, but some viruses are able to detect bacteria population density, which appears to affect the frequency of lysogeny (Hargreaves et al., 2014; Silpe and Bassler, 2018). If this process applies to *P. aeruginosa* and its viruses, a more sophisticated model would incorporate a density-dependent latency probability: $f_T(N)$ and $f_C(N)$.

Finally, in deducing the expected chronic lysogen frequency f_C and the recovery (cure) rates γ , we have assumed that all other parameters are exactly the baselines given in Table 2. While the literature has provided reasonable ranges for these parameters, several baseline values (e.g., β_C , η_T , and η_C) were simply selected within those ranges. Given the uncertainty in several parameter values, the model-inferred parameters f_C and γ are also uncertain.

4.3. Future steps

This model could serve as a base for more sophisticated extensions. For instance, the presented model does not include an evolutionary component and is therefore only applicable on short time scales. However, this model could be part of a multi-scale model that incorporates both short time-scale (ecological) dynamics and long time-scale (evolutionary) dynamics.

Also, we have assumed that no environmental stressors (e.g., radiation, heat, sublethal antibiotics) perturb the system, but antibiotics are often used to treat bacterial infections. Many classes of antibiotics are known to induce latent proviruses and trigger virus production, even if the bacteria are antibiotic resistant (Rokney et al., 2008; Fothergill et al., 2011; López et al., 2014; Martínez-García et al., 2015; Kaur et al., 2012). In fact, the induction of latent viruses is proposed to be one of the mechanisms behind the synergistic effect of antibiotics and viruses to treat recalcitrant bacterial infections (Kaur et al., 2012; Kim et al., 2018). Infections by *P. aeruginosa* represent about 10% of nosocomial infections, are a leading cause of death among patients with cystic fibrosis, and have been deemed a serious threat on the United States Centers for Disease Control watch list for antibiotic resistance (Jarvis and Martone, 1992; Hancock and Speert, 2000; US Department of Health and Human Services, 2013); therefore, a critical next step is understanding the impact of antibiotic-induced proviruses on control of bacterial infections. This is the subject of ongoing study.

5. Conclusion

We have developed a simple mathematical model of the ecological competition between temperate and chronic viruses for bacterial hosts. Using the hosts *E. coli* and *P. aeruginosa* as motivation, we demonstrate that low lysogen frequencies provide competitive advantages for both viral types. Interestingly, chronic viruses theoretically maximize their steady state density by eliminating latency entirely, but temperate viruses exhibit a non-zero 'sweet spot' lysogen frequency. Using experimental evidence that temperate viruses possess lysogen frequencies around 1% and that both viral types coexist in real environments, we are able to estimate the recovery (cure) rates for bacteria. Better understanding of this system may contribute to optimal treatment of bacterial infections using phage therapy and/or antibiotics.

6. Data availability

All software (Matlab.m files) are publicly available via the Illinois Data Bank (Rapti, Z., 2021) (https://doi.org/10.13012/B21DB-0705058_V1).

CRedit authorship contribution statement

Sara M. Clifton: Conceptualization, Methodology, Software, Validation, Writing - original draft, Writing - review & editing, Visualization. **Rachel J. Whitaker:** Conceptualization, Validation, Writing - review & editing, Funding acquisition. **Zoi Rapti:** Conceptualization, Methodology, Software, Validation, Formal analysis, Writing - original draft, Writing - review & editing, Visualization, Funding acquisition.

Declaration of Competing Interest

The authors declare that they have no known competing financial interests or personal relationships that could have appeared to influence the work reported in this paper.

Acknowledgements

This work was funded in part by the National Science Foundation grant DMS-1815764 (ZR), the Cystic Fibrosis Foundation grant WHITAK16PO (RJW), and an Allen Distinguished Investigator Award (RJW). The funders had no role in study design, data collection and analysis, decision to publish, or preparation of the manuscript.

The authors thank Jayadevi H. Chandrashekar and George A. O'Toole for discussions that informed biological aspects of this work. Thanks are also due to Ted Kim and Karna Gowda for assistance with parameter selection. The authors also thank two anonymous reviewers for insightful comments that greatly improved the clarity of the article.

Appendix A. Steady states

The following biologically relevant steady-states exist for system (1)–(7).

- First, it can be readily seen that the trivial steady state, where all population densities are zero, exists.
- Second, the steady state where only the susceptible class persists and is equal to the bacterial carrying capacity, $S = K$, also exists for all parameter values.
- The steady state where only the temperate phage persists, namely $P_C = V_C = L_C = 0$, also exists. In this case it holds:

$$\begin{aligned} S &= \frac{\mu_T}{\eta_T} \frac{\delta + \gamma_I}{\beta_T \delta (1 - f_T) - (\delta + \gamma_I)} \\ V_T &= \frac{\beta_T \delta (1 - f_T) - (\delta + \gamma_I)}{\mu_T (1 - f_T)} I_T \\ I_T &= \frac{S(1 - S)(1 - f_T)}{(S - \gamma_I)(1 - f_T) + (\delta + \gamma_I)} + \frac{(1 - f_T)(\gamma_T - S)}{(S - \gamma_I)(1 - f_T) + (\delta + \gamma_I)} L_T \\ r_T((\gamma_T - \gamma_I)(1 - f_T) + \delta + \gamma_I) L_T^2 &+ (\gamma_T(1 - f_T)(S + \delta) \\ &+ (\delta + \gamma_I) f_T S - (\delta + f_T \gamma_I) r_T(1 - S)) L_T - f_T(\delta + \gamma_I) S(1 - S) \\ &= 0 \end{aligned}$$

- Similarly, when only the chronic phage persists, namely when $I_T = V_T = L_T = 0$, it holds

$$\begin{aligned} S &= \frac{\mu_C}{\eta_C} \frac{\gamma_P}{\beta_C(1 - f_C) - \gamma_P} \\ P_C &= \frac{1 - S}{1 + \frac{f_C \gamma_P}{(1 - f_C) \gamma_C}} \\ L_C &= \frac{f_C \gamma_P}{(1 - f_C) \gamma_C} P_C \\ V_C &= \frac{\beta_C(1 - f_C) - \gamma_P}{\mu_C(1 - f_C)} P_C \end{aligned}$$

- Finally, if all population densities are positive, it holds

$$\begin{aligned}
 S &= \frac{\mu_T}{\eta_T} \frac{\delta + \gamma_I}{\beta_T \delta (1 - f_T) - (\delta + \gamma_I)} \\
 1 - N &= \frac{\gamma_P}{r_P} - \frac{(1 - f_C) \beta_C}{r_P} - \frac{\eta_C S}{\eta_C S + \mu_C} \\
 V_T &= \frac{\beta_T \delta (1 - f_T) - (\delta + \gamma_I)}{\mu_T (1 - f_T)} I_T \\
 V_C &= \frac{\beta_C}{\eta_C S + \mu_C} P_C \\
 L_T &= \frac{f_T}{1 - f_T} \frac{\delta + \gamma_I}{\gamma_T - r_T (1 - N)} I_T \\
 L_C &= \frac{\eta_C f_C \beta_C S}{\eta_C S + \mu_C} \frac{1}{\gamma_C - r_C (1 - N)} P_C.
 \end{aligned}$$

The following linear 2×2 system can be solved to yield a unique steady-state.

$$\begin{aligned}
 &\left(\frac{\delta + \gamma_I}{1 - f_T} \frac{\gamma_T (1 - f_T) - r_T (1 - N)}{\gamma_T - r_T (1 - N)} - \gamma_I \right) I_T \\
 &+ \left(\frac{\eta_C \beta_C S}{\eta_C S + \mu_C} \frac{\gamma_C (1 - f_C) - r_C (1 - N)}{\gamma_C - r_C (1 - N)} - \gamma_P \right) P_C = S(1 - N) \\
 &\left(1 + \frac{f_T}{1 - f_T} \frac{\delta + \gamma_I}{\gamma_T - r_T (1 - N)} \right) I_T \\
 &+ \left(1 + \frac{\eta_C f_C \beta_C S}{\eta_C S + \mu_C} \frac{1}{\gamma_C - r_C (1 - N)} \right) P_C = N - S
 \end{aligned}$$

Appendix B. Viral invasion fitness

The basic reproductive number R_0 , traditionally defined as the average number of new infections generated by an infectious individual in an entirely susceptible population [Diekmann et al., 1990](#), has long been used to characterize a pathogen's fitness [Rapti and Cáceres, 2016](#); [Weitz et al., 2019](#); [Andreasen and Pugliese, 1995](#); [Adams and Sasaki, 2007](#)). The basic reproductive number has been found to be correlated with the between-host transmission rate [Beretta and Kuang, 1998](#), the number of free infective propagules produced per infected host (virions, in our case), and life-history traits such as mortality, fecundity, and growth [Rapti and Cáceres, 2016](#); [Gilchrist et al., 2006](#).

In this study, R_0 is used to determine the growth rate of a viral invader in a population of residents at steady state. Specifically, when either the temperate or chronic virus attempts to invade the bacterial population, the virus is successful when its respective R_0 is greater than one. Similarly, when one of the two viruses is the resident, the other virus can invade and coexist as long as its R_0 is greater than one. The various regions where each virus invades and persists are shown in [Fig. 4](#).

One of the goals and challenges of phage therapy is to ensure that there is active viral replication [Payne and Jansen, 2001](#). This occurs when, after an initial dose of the virus, it is able to proliferate in its bacterial host. There are cases however, when viral replication does not take place, so repeated administration of the virus is required. There already exist various models that study viral kinetics and provide thresholds that guarantee active replication of lytic-only viruses [Payne and Jansen, 2001](#); [Payne and Jansen, 2003](#). Yet, as in most models, recovery of the bacterial host is neglected.

Given the large range of recovery rates that viruses exhibit [Brüssow et al., 2004](#); [Horvath and Barrangou, 2010](#), in this work, we investigate and identify viral recovery strategies that optimize viral abundance. Although the basic reproductive number is a traditional measure of fitness (see e.g., [Wahl et al., 2019](#)), using abundance as a proxy for competitive advantage is also common (see e.g., [Thingstad et al., 2014](#)).

Appendix C. Linear stability analysis and bifurcations

1. The trivial equilibrium is linearly unstable for all choices of parameter values.
2. The steady-state with $S = 1$ is linearly stable as long as

$$R_T = \frac{(1 - f_T) \eta_T \beta_T \delta}{(\mu_T + \eta_T) (\delta + \gamma_I)} < 1, \quad R_C = \frac{(1 - f_C) \eta_C \beta_C}{\gamma_P (\mu_C + \eta_C)} < 1.$$

We notice from the previous section that when $S = 1$ it holds

$$S = \frac{\mu_T}{\eta_T} \frac{\delta + \gamma_I}{\beta_T \delta (1 - f_T) - (\delta + \gamma_I)} = 1 \iff R_T = 1$$

and

$$S = \frac{\mu_C}{\eta_C} \frac{\gamma_P}{\beta_C (1 - f_C) - \gamma_P} = 1 \iff R_C = 1.$$

Therefore, the susceptible only ($S = 1$) steady-state undergoes a transcritical bifurcation with the $P_C = V_C = L_C = 0$ (temperate only) steady state when $R_T = 1$. Similarly, it undergoes a transcritical bifurcation with the $I_T = V_T = L_T = 0$ (chronic only) steady state when $R_C = 1$.

3. The temperate only steady state undergoes a transcritical bifurcation with the coexistence steady state when

$$R_{TC} = \frac{(1 - f_C) \beta_C \eta_C S}{\eta_C S + \mu_C} \frac{1}{\gamma_P - r_P (1 - N)} = 1,$$

$$\text{where } S = \frac{\mu_T}{\eta_T} \frac{\delta + \gamma_I}{\beta_T \delta (1 - f_T) - (\delta + \gamma_I)} \text{ and } N = S + I_T + L_T.$$

4. There is a transcritical bifurcation from the chronic only to the coexistence steady-state when

$$R_{CT} = \frac{(1 - f_T) \beta_T \delta \eta_T S}{(\eta_T S + \mu_T) (\delta + \gamma_I)} = 1, \quad \text{where } S = \frac{\mu_C}{\eta_C} \frac{\gamma_P}{\beta_C (1 - f_C) - \gamma_P}.$$

All these bifurcations are obtained by a standard linear stability analysis around the relevant steady states.

Appendix D. Model rescaling

The dimensional model system [\(D.1\)–\(D.7\)](#) below can be rescaled so that time and bacterial density are unitless quantities. Although the viral density can also be nondimensionalized to be unitless, we have elected (for the sake of interpretability) to rescale viral density to have units of PFU/CFU.

$$\dot{\tilde{S}} = \tilde{r}_S \tilde{S} \underbrace{\left(1 - \frac{\tilde{N}}{\tilde{K}} \right)}_{\text{growth}} - \underbrace{\tilde{\eta}_T \tilde{S} \tilde{V}_T - \tilde{\eta}_C \tilde{S} \tilde{V}_C}_{\text{infection}} + \underbrace{\tilde{\gamma}_T \tilde{L}_T + \tilde{\gamma}_I \tilde{I}_T + \tilde{\gamma}_P \tilde{P}_C + \tilde{\gamma}_C \tilde{L}_C}_{\text{recovery}} \tag{D.1}$$

$$\dot{\tilde{I}}_T = \underbrace{\tilde{\eta}_T (1 - \tilde{f}_T) \tilde{S} \tilde{V}_T}_{\text{infection}} - \underbrace{\tilde{\delta} \tilde{I}_T}_{\text{lysis}} - \underbrace{\tilde{\gamma}_I \tilde{I}_T}_{\text{recovery}} \tag{D.2}$$

$$\dot{\tilde{L}}_T = \tilde{r}_T \tilde{L}_T \underbrace{\left(1 - \frac{\tilde{N}}{\tilde{K}} \right)}_{\text{growth}} + \underbrace{\tilde{\eta}_T \tilde{f}_T \tilde{S} \tilde{V}_T}_{\text{infection}} - \underbrace{\tilde{\gamma}_T \tilde{L}_T}_{\text{recovery}} \tag{D.3}$$

$$\dot{\tilde{P}}_C = \tilde{r}_P \tilde{P}_C \underbrace{\left(1 - \frac{\tilde{N}}{\tilde{K}} \right)}_{\text{growth}} + \underbrace{(1 - \tilde{f}_C) \tilde{\eta}_C \tilde{S} \tilde{V}_C}_{\text{infection}} - \underbrace{\tilde{\gamma}_P \tilde{P}_C}_{\text{recovery}} \tag{D.4}$$

$$\dot{\tilde{L}}_C = \tilde{r}_C \tilde{L}_C \underbrace{\left(1 - \frac{\tilde{N}}{\tilde{K}} \right)}_{\text{growth}} + \underbrace{\tilde{f}_C \tilde{\eta}_C \tilde{S} \tilde{V}_C}_{\text{infection}} - \underbrace{\tilde{\gamma}_C \tilde{L}_C}_{\text{recovery}} \tag{D.5}$$

$$\dot{\tilde{V}}_T = \underbrace{\tilde{\beta}_T \tilde{\delta} \tilde{I}_T}_{\text{burst}} - \underbrace{\tilde{\eta}_T \tilde{S} \tilde{V}_T}_{\text{adsorption}} - \underbrace{\tilde{\mu}_T \tilde{V}_T}_{\text{degradation}} \tag{D.6}$$

$$\dot{\tilde{V}}_C = \underbrace{\tilde{\beta}_C \tilde{P}_C}_{\text{production}} - \underbrace{\tilde{\eta}_C \tilde{S} \tilde{V}_C}_{\text{adsorption}} - \underbrace{\tilde{\mu}_C \tilde{V}_C}_{\text{degradation}} \tag{D.7}$$

Suppose Eqs. (D.1)–(D.7) have bacterial density units of CFU/mL, viral density units of PFU/mL, and time units of minutes; then Eqs. (D.1)–(D.5) have units of CFU/mL/min, and Eqs. (D.6) and (D.7) have units of PFU/mL/min. We will make the following substitutions into the system:

$$\begin{aligned}\tilde{S} &= \tilde{K} S & \tilde{I}_T &= \tilde{K} I_T \\ \tilde{L}_T &= \tilde{K} L_T & \tilde{P}_C &= \tilde{K} P_C \\ \tilde{L}_C &= \tilde{K} L_C & \tilde{N} &= \tilde{K} N \\ \tilde{V}_T &= \tilde{K} V_T & \tilde{V}_C &= \tilde{K} V_C \\ \tilde{t} &= \frac{t}{\tilde{r}_S}\end{aligned}$$

where S, \dots, N are unitless bacterial densities, V_T, V_C have units of PFU/CFU (a virus to bacteria ratio), and t is a unitless time. An alternate substitution of $\tilde{V}_T = \tilde{\beta}_T \tilde{K} V_T$ and $\tilde{V}_C = \tilde{\beta}_C \tilde{K} V_C$ would have led to a nondimensionalization of the system, but the nondimensionalized viral densities would have been more challenging to interpret; therefore we eschew this option.

We will illustrate the rescaling process for bacterial dynamics with Eq. (D.1), and Eqs. (D.2)–(D.5) are similar:

$$\frac{d\tilde{S}}{d\tilde{t}} = \underbrace{\tilde{r}_S \tilde{S} \left(1 - \frac{\tilde{N}}{\tilde{K}}\right)}_{\text{growth}} - \underbrace{\tilde{\eta}_T \tilde{S} \tilde{V}_T - \tilde{\eta}_C \tilde{S} \tilde{V}_C}_{\text{infection}} + \underbrace{\tilde{\gamma}_T \tilde{L}_T + \tilde{\gamma}_I \tilde{I}_T + \tilde{\gamma}_P \tilde{P}_C + \tilde{\gamma}_C \tilde{L}_C}_{\text{recovery}}$$

After making the substitutions into Eq. (D.1), we get

$$\begin{aligned}\frac{d(\tilde{K}S)}{d(t/\tilde{r}_S)} &= \underbrace{\tilde{r}_S \tilde{K} S \left(1 - \frac{\tilde{K}N}{\tilde{K}}\right)}_{\text{growth}} - \underbrace{\tilde{\eta}_T \tilde{K} S \tilde{K} V_T - \tilde{\eta}_C \tilde{K} S \tilde{K} V_C}_{\text{infection}} \\ &+ \underbrace{\tilde{\gamma}_T \tilde{K} L_T + \tilde{\gamma}_I \tilde{K} I_T + \tilde{\gamma}_P \tilde{K} P_C + \tilde{\gamma}_C \tilde{K} L_C}_{\text{recovery}}\end{aligned}$$

We now divide the equation by $\tilde{K} \tilde{r}_S$:

$$\frac{dS}{d\tilde{t}} = \underbrace{S(1-N)}_{\text{growth}} - \underbrace{\frac{\tilde{\eta}_T \tilde{K}}{\tilde{r}_S} S V_T - \frac{\tilde{\eta}_C \tilde{K}}{\tilde{r}_S} S V_C}_{\text{infection}} + \underbrace{\frac{\tilde{\gamma}_T}{\tilde{r}_S} L_T + \frac{\tilde{\gamma}_I}{\tilde{r}_S} I_T + \frac{\tilde{\gamma}_P}{\tilde{r}_S} P_C + \frac{\tilde{\gamma}_C}{\tilde{r}_S} L_C}_{\text{recovery}}$$

The transformed parameters are now evident:

$$\begin{aligned}\eta_T &= \frac{\tilde{\eta}_T \tilde{K}}{\tilde{r}_S} & \eta_C &= \frac{\tilde{\eta}_C \tilde{K}}{\tilde{r}_S} \\ \gamma_T &= \frac{\tilde{\gamma}_T}{\tilde{r}_S} & \gamma_I &= \frac{\tilde{\gamma}_I}{\tilde{r}_S} \\ \gamma_P &= \frac{\tilde{\gamma}_P}{\tilde{r}_S} & \gamma_C &= \frac{\tilde{\gamma}_C}{\tilde{r}_S}\end{aligned}$$

Eq. (D.1) reduces to

$$\frac{dS}{d\tilde{t}} = \underbrace{S(1-N)}_{\text{growth}} - \underbrace{\eta_T S V_T - \eta_C S V_C}_{\text{infection}} + \underbrace{\gamma_T L_T + \gamma_I I_T + \gamma_P P_C + \gamma_C L_C}_{\text{recovery}}$$

Eqs. (D.2)–(D.5) are rescaled in a similar manner. Substituting the transformations into Eqs. (D.6) and (D.7) yields

$$\begin{aligned}\frac{d(\tilde{K}V_T)}{d(t/\tilde{r}_S)} &= \underbrace{\tilde{\beta}_T \tilde{\delta} \tilde{K} I_T}_{\text{burst}} - \underbrace{\tilde{\eta}_T \tilde{K} S \tilde{K} V_T}_{\text{adsorption}} - \underbrace{\tilde{\mu}_T \tilde{K} V_T}_{\text{degradation}} \\ \frac{d(\tilde{K}V_C)}{d(t/\tilde{r}_S)} &= \underbrace{\tilde{\beta}_C \tilde{K} P_C}_{\text{production}} - \underbrace{\tilde{\eta}_C \tilde{K} S \tilde{K} V_C}_{\text{adsorption}} - \underbrace{\tilde{\mu}_C \tilde{K} V_C}_{\text{degradation}}\end{aligned}$$

Again dividing by $\tilde{K} \tilde{r}_S$, we get:

$$\begin{aligned}\frac{dV_T}{d\tilde{t}} &= \underbrace{\tilde{\beta}_T \frac{\tilde{\delta}}{\tilde{r}_S} I_T}_{\text{burst}} - \underbrace{\frac{\tilde{\eta}_T \tilde{K}}{\tilde{r}_S} S V_T}_{\text{adsorption}} - \underbrace{\frac{\tilde{\mu}_T}{\tilde{r}_S} V_T}_{\text{degradation}} \\ \frac{dV_C}{d\tilde{t}} &= \underbrace{\frac{\tilde{\beta}_C}{\tilde{r}_S} P_C}_{\text{production}} - \underbrace{\frac{\tilde{\eta}_C \tilde{K}}{\tilde{r}_S} S V_C}_{\text{adsorption}} - \underbrace{\frac{\tilde{\mu}_C}{\tilde{r}_S} V_C}_{\text{degradation}}\end{aligned}$$

Adding to our list of transformed parameters

$$\begin{aligned}\beta_T &= \tilde{\beta}_T & \beta_C &= \frac{\tilde{\beta}_C}{\tilde{r}_S} \\ \mu_T &= \frac{\tilde{\mu}_T}{\tilde{r}_S} & \mu_C &= \frac{\tilde{\mu}_C}{\tilde{r}_S} \\ \delta &= \frac{\tilde{\delta}}{\tilde{r}_S}\end{aligned}$$

the viral density equations reduce to

$$\begin{aligned}\frac{dV_T}{d\tilde{t}} &= \underbrace{\beta_T \delta I_T}_{\text{burst}} - \underbrace{\eta_T S V_T}_{\text{adsorption}} - \underbrace{\mu_T V_T}_{\text{degradation}} \\ \frac{dV_C}{d\tilde{t}} &= \underbrace{\beta_C P_C}_{\text{production}} - \underbrace{\eta_C S V_C}_{\text{adsorption}} - \underbrace{\mu_C V_C}_{\text{degradation}}\end{aligned}$$

The full set of transformed parameters is listed in Table D.3.

Appendix E. Parameter selection

The **growth rate** \tilde{r}_S for *P. aeruginosa in vitro* is approximately $5.1e-3 \text{ min}^{-1}$ (Spalding et al., 2018), although *P. aeruginosa* growth is highly variable in humans (Kopf et al., 2016). Therefore all rate parameters provided in min^{-1} are divided by this rate in order to rescale (see Table D.3).

The growth rates for latently infected bacteria, \tilde{r}_T and \tilde{r}_C , are assumed to be similar to uninfected bacteria. Our estimate for the growth rate \tilde{r}_P of productive bacteria is based on *E. coli* infected with the filamentous phage M13 (Shapiro et al., 2016); depending on the experimentally imposed fitness pressure, chronic viruses appear capable of either increasing or decreasing host growth rates. In the interest of simplicity, we assumed that chronic bacteria grow at a rate similar to uninfected bacteria.

The **carrying capacity** \tilde{K} of bacteria in a medium depends on the environment. Even within the sputum of patients with cystic fibrosis, the carrying capacity is difficult to estimate due to variability among patients. One study of patients with cystic fibrosis found that the densities of viable *P. aeruginosa* in sputum of 12 patients not undergoing treatment ranged from $5.3e3 \text{ CFU/mL}$ to $1.8e11 \text{ CFU/mL}$ (Stressmann et al., 2011). Because of the wide range of carrying capacities, we use the geometric mean of this range, $3e7 \text{ CFU/mL}$, for illustrative purposes only. Because \tilde{K} is challenging to estimate, we use strategies that do not explicitly require \tilde{K} to estimate the infection rate.

The **infection rate** for *E. coli* and T4 phage in mucus (assuming mass action infection) is known to be approximately $47e-10 \text{ mL/min}$ per PFU (Stent et al., 1963; Barr et al., 2015). Infection in marine ecosystems (also assuming mass action infection) is similar at around $24e-10 \text{ mL/min}$ per PFU (Stent et al., 1963; Thingstad et al., 2014). Given our uncertainty in the bacterial carrying capacity, we elect to use an infection rate within the range given by Sinha et al. (2017); the authors fit their mass action infection model to time series population data that reached carrying capacity. The authors present $\tilde{K} \tilde{\eta} \in [0.45, 100] \text{ hr}^{-1}$ and $\tilde{r}_S \in [0.5, 10] \text{ hr}^{-1}$. Rescaling leads to a range of η between 0.045 and 200, and our selected value of $\eta = 1$ is near the geometric mean of that range.

Table D.3
Summary of model parameter groupings after rescaling of system (D.1)–(D.7).

Parameter	Units	Associated parameter grouping	Units
\bar{r}_S	min^{-1}	$r_S = \frac{\bar{r}_S}{\bar{r}_S} = 1$	unitless
$\bar{r}_T, \bar{r}_P, \bar{r}_C$	min^{-1}	$r_T = \frac{\bar{r}_T}{\bar{r}_S}, r_P = \frac{\bar{r}_P}{\bar{r}_S}, r_C = \frac{\bar{r}_C}{\bar{r}_S}$	unitless
\tilde{K}	$\frac{\text{CFU}}{\text{mL}}$	$K = \frac{\tilde{K}}{K} = 1$	unitless
$\tilde{\eta}_T, \tilde{\eta}_C$	$\frac{\text{mL}}{\text{PFUmin}}$	$\eta_T = \frac{\tilde{\eta}_T \tilde{K}}{\bar{r}_S}, \eta_C = \frac{\tilde{\eta}_C \tilde{K}}{\bar{r}_S}$	$\frac{\text{CFU}}{\text{PFU}}$
$\tilde{\gamma}_T, \tilde{\gamma}_I, \tilde{\gamma}_P, \tilde{\gamma}_C$	min^{-1}	$\gamma_T = \frac{\tilde{\gamma}_T}{\bar{r}_S}, \gamma_I = \frac{\tilde{\gamma}_I}{\bar{r}_S}, \gamma_P = \frac{\tilde{\gamma}_P}{\bar{r}_S}, \gamma_C = \frac{\tilde{\gamma}_C}{\bar{r}_S}$	unitless
$\tilde{\delta}$	min^{-1}	$\delta = \frac{\tilde{\delta}}{\bar{r}_S}$	unitless
\tilde{f}_T	unitless	$f_T = \tilde{f}_T$	unitless
\tilde{f}_C	unitless	$f_C = \tilde{f}_C$	unitless
$\tilde{\beta}_T$	$\frac{\text{PFU}}{\text{CFU}}$	$\beta_T = \tilde{\beta}_T$	$\frac{\text{PFU}}{\text{CFU}}$
$\tilde{\beta}_C$	$\frac{\text{PFU}}{\text{CFUmin}}$	$\beta_C = \frac{\tilde{\beta}_C}{\bar{r}_S}$	$\frac{\text{PFU}}{\text{CFU}}$
$\tilde{\mu}_T, \tilde{\mu}_C$	min^{-1}	$\mu_T = \frac{\tilde{\mu}_T}{\bar{r}_S}, \mu_C = \frac{\tilde{\mu}_C}{\bar{r}_S}$	unitless

The **phage production delay rate** $\tilde{\delta}$ is estimated based on the eclipse and rise phase of PAXYB1 and ϕ PSZ1 phage (Yu et al., 2017; El Didamony et al., 2015). The eclipse (latent) and rise phase is 130 min total for PAXYB1 (Yu et al., 2017) and 27 min total for ϕ PSZ1 (El Didamony et al., 2015). The smallest (nondimensional) delay rate is then $1/130/5.1e-3 = 1.5$, and the largest is $1/27/5.1e-3 = 7.3$. We selected the approximate average of this range, 4, to be the delay rate δ .

The **temperate lysogen frequency** f_T is estimated based on *E. coli* and λ phage (Oppenheim and Adhya, 2007): “It is known that a cell infected by one phage predominantly follows the lytic default pathway (about 99% of the time).”

The **phage degradation rates** $\tilde{\mu}_T$ and $\tilde{\mu}_C$ were estimated based on the decay rates of phage in aquatic environments (Heldal and Bratbak, 1991). The decay rates ranged from 0.26 to 1.1 per hour. We nondimensionalize by multiplying by 60 min per hour and the bacterial growth rate, $5.1e-3$ per minute. The nondimensional range of decay rates is then 0.9 to 3.6. We selected a value of $\mu_T = \mu_C = 1$ arbitrarily from this range.

All other parameter baselines and ranges are educated guesses.

References

Adams, B., Sasaki, A., 2007. Cross-immunity, invasion and coexistence of pathogen strains in epidemiological models with one-dimensional antigenic space. *Mathematical Biosciences* 210 (2), 680–699.

Altamirano, F.L.G., Barr, J.J., 2019. Phage therapy in the postantibiotic era. *Clinical Microbiology Reviews* 32 (2), e00066–18.

Andreasen, V., Pugliese, A., 1995. Pathogen coexistence induced by density-dependent host mortality. *Journal of Theoretical Biology* 177 (2), 159–165.

Barr, J.J., Auro, R., Sam-Soon, N., Kassegne, S., Peters, G., Bonilla, N., Hatay, M., Mourrada, S., Bailey, B., Youle, M., 2015. Subdiffusive motion of bacteriophage in mucosal surfaces increases the frequency of bacterial encounters. *Proceedings of the National Academy of Sciences* 112 (44), 13675–13680.

Beretta, E., Kuang, Y., 1998. Modeling and analysis of a marine bacteriophage infection. *Mathematical Biosciences* 149, 57–76.

Brüssow, H., Canchaya, C., Hardt, W.-D., 2004. Phages and the evolution of bacterial pathogens: from genomic rearrangements to lysogenic conversion. *Microbiology and Molecular Biology Reviews* 68 (3), 560–602.

Calendar, R., 2006. *The Bacteriophages*. Oxford University Press on Demand.

Casjens, S., 2003. Prophages and bacterial genomics: what have we learned so far? *Molecular Microbiology* 49 (2), 277–300.

Ceyssens, P.-J., Brabban, A., Rogge, L., Lewis, M.S., Pickard, D., Goulding, D., Dougan, G., Noben, J.-P., Kropinski, A., Kutter, E., et al., 2010. Molecular and physiological analysis of three pseudomonas aeruginosa phages belonging to the ‘n4-like viruses’. *Virology* 405 (1), 26–30.

Clifton, S.M., Kim, T., Chandrashekar, J.H., O’Toole, G.A., Rapti, Z., Whitaker, R.J., 2019. Lying in wait: Modeling the control of bacterial infections via antibiotic-induced proviruses. *MSystems* 4 (5), e00221–19.

Comeau, A.M., Tétart, F., Trojet, S.N., Prere, M.-F., Krisch, H., 2007. Phage-antibiotic synergy (pas): β -lactam and quinolone antibiotics stimulate virulent phage growth. *PLoS One* 2 (8), e799.

Cortes, M.G., Krog, J., Balazsi, G., 2019. Optimality of the spontaneous prophage induction rate, bioRxiv. arXiv:https://www.biorxiv.org/content/early/2019/02/

11/546275.full.pdf, doi:10.1101/546275. URL: https://www.biorxiv.org/content/early/2019/02/11/546275..

Courtney, J., Bradley, J., McCaughan, J., O’connor, T., Shortt, C., Bredin, C., Bradbury, I., Elborn, J., 2007. Predictors of mortality in adults with cystic fibrosis. *Pediatric Pulmonology* 42 (6), 525–532.

Davies, E.V., Winstanley, C., Fothergill, J.L., James, C.E., 2016. The role of temperate bacteriophages in bacterial infection. *FEMS Microbiology Letters* 363 (5).

De Smet, J., Hendrix, H., Blasdel, B.G., Danis-Wlodarczyk, K., Lavigne, R., 2017. Pseudomonas predators: Understanding and exploiting phage–host interactions. *Nature Reviews Microbiology* 15 (9), 517.

Diekmann, O., Heesterbeek, J., Metz, J., 1990. On the definition and the computation of the basic reproduction ratio r_0 in models of infectious diseases in heterogeneous population. *Journal of Mathematical Biology* 28, 365–382.

Dimmock, N.J., Easton, A.J., Leppard, K.N., 2016. *Introduction to Modern Virology*. John Wiley & Sons.

El Didamony, G., Askora, A., Shehata, A.A., 2015. Isolation and characterization of t7-like lytic bacteriophages infecting multidrug resistant pseudomonas aeruginosa isolated from egypt. *Current Microbiology* 70 (6), 786–791.

Emerson, J., Rosenfeld, M., McNamara, S., Ramsey, B., Gibson, R.L., 2002. Pseudomonas aeruginosa and other predictors of mortality and morbidity in young children with cystic fibrosis. *Pediatric Pulmonology* 34 (2), 91–100.

Fothergill, J.L., Mowat, E., Walshaw, M.J., Ledson, M.J., James, C.E., Winstanley, C., 2011. Effect of antibiotic treatment on bacteriophage production by a cystic fibrosis epidemic strain of pseudomonas aeruginosa. *Antimicrobial Agents and Chemotherapy* 55 (1), 426–428.

Garbe, J., Bunk, B., Rohde, M., Schobert, M., 2011. Sequencing and characterization of pseudomonas aeruginosa phage jg004. *BMC Microbiology* 11 (1), 102.

Garro, A.J., Law, M.-F., 1974. Relationship between lysogeny, spontaneous induction, and transformation efficiencies in bacillus subtilis. *Journal of Bacteriology* 120 (3), 1256–1259.

Gilchrist, M.A., Sulsky, D., Pringle, A., 2006. Identifying fitness and optimal life-history strategies for an asexual filamentous fungus. *Evolution* 60, 970–979.

Gulbudak, H., Weitz, J.S., 2019. Heterogeneous viral strategies promote coexistence in virus–microbe systems. *Journal of Theoretical Biology* 462, 65–84.

Hancock, R.E., Speert, D.P., 2000. Antibiotic resistance in pseudomonas aeruginosa: mechanisms and impact on treatment. *Drug Resistance Updates* 3 (4), 247–255.

Hargreaves, K.R., Kropinski, A.M., Clokie, M.R., 2014. What does the talking?: Quorum sensing signalling genes discovered in a bacteriophage genome. *PLoS One* 9 (1), e85131.

Harper, D.R., Parracho, H.M., Walker, J., Sharp, R., Hughes, G., Werthén, M., Lehman, S., Morales, S., 2014. Bacteriophages and biofilms. *Antibiotics* 3 (3), 270–284.

Heldal, M., Bratbak, G., 1991. Production and decay of viruses in aquatic environments. *Marine Ecology Progress Series*, 205–212.

Heo, Y.-J., Chung, I.-Y., Choi, K.B., Lau, G.W., Cho, Y.-H., 2007. Genome sequence comparison and superinfection between two related pseudomonas aeruginosa phages, d3112 and mp22. *Microbiology* 153 (9), 2885–2895.

Hobbs, Z., Abedon, S.T., 2016. Diversity of phage infection types and associated terminology: the problem with lytic or lysogenic. *FEMS Microbiology Letters* 363 (7).

Horvath, P., Barrangou, R., 2010. Crispr/cas, the immune system of bacteria and archaea. *Science* 327 (5962), 167–170.

James, C.E., Fothergill, J.L., Kalwij, H., Hall, A.J., Cottell, J., Brockhurst, M.A., Winstanley, C., 2012. Differential infection properties of three inducible prophages from an epidemic strain of pseudomonas aeruginosa. *BMC Microbiology* 12 (1), 216.

James, C.E., Davies, E.V., Fothergill, J.L., Walshaw, M.J., Beale, C.M., Blockhurst, M.A., Winstanley, C., 2015. Lytic activity by temperate phages of pseudomonas aeruginosa in long-term cystic fibrosis chronic lung infections. *The ISME Journal* 9, 1391–1398.

Jarvis, W.R., Martone, W.J., 1992. Predominant pathogens in hospital infections. *Journal of Antimicrobial Chemotherapy* 29 (suppl_A), 19–24.

Kaur, S., Harjai, K., Chhibber, S., 2012. Plaque-size enhancement of mrsa phages using sub-lethal concentrations of antibiotics. *Applied and Environmental Microbiology* AEM-02371..

Kim, M., Jo, Y., Hwang, Y.J., Hong, H.W., Hong, S.S., Park, K., Myung, H., 2018. Phage-antibiotic synergy via delayed lysis. *Applied and Environmental Microbiology* 84 (22), e02085–18.

Knowles, B., Silveira, C., Bailey, B., Barott, K., Cantu, V., Cobián-Güemes, A., Coutinho, F., Dinsdale, E., Felts, B., Furby, K., et al., 2016. Lytic to temperate switching of viral communities. *Nature* 531 (7595), 466.

Kopf, S.H., Sessions, A.L., Cowley, E.S., Reyes, C., Van Sambeek, L., Hu, Y., Orphan, V.J., Kato, R., Newman, D.K., 2016. Trace incorporation of heavy water reveals slow and heterogeneous pathogen growth rates in cystic fibrosis sputum. *Proceedings of the National Academy of Sciences* 113 (2), E110–E116.

Kung, V.L., Ozer, E.A., Hauser, A.R., 2010. The accessory genome of pseudomonas aeruginosa. *Microbiology and Molecular Biology Reviews* 74 (4), 621–641.

Kutter, E., De Vos, D., Gvasalia, G., Alavidze, Z., Gogokhia, L., Kuhl, S., Abedon, S.T., 2010. Phage therapy in clinical practice: treatment of human infections. *Current Pharmaceutical Biotechnology* 11 (1), 69–86.

Latino, L., Essoh, C., Blouin, Y., Thien, H.V., Poursel, C., 2014. A novel pseudomonas aeruginosa bacteriophage, ab31, a chimera formed from temperate phage paju2 and p. putida lytic phage af: characteristics and mechanism of bacterial resistance. *PLoS One* 9(4):e93777..

Lin, Y., Chang, R.Y.K., Britton, W.J., Morales, S., Kutter, E., Chan, H.-K., 2018. Synergy of nebulized phage pev20 and ciprofloxacin combination against pseudomonas aeruginosa. *International Journal of Pharmaceutics* 551 (1–2), 158–165.

- López, E., Domenech, A., Ferrándiz, M.-J., Frias, M.J., Ardanuy, C., Ramirez, M., García, E., Liñares, J., Adela, G., 2014. Induction of prophages by fluoroquinolones in streptococcus pneumoniae: implications for emergence of resistance in genetically-related clones. *PLoS One* 9, (4) e94358.
- Lwoff, A., 1953. Lysogeny. *Bacteriological Reviews* 17 (4), 269.
- Martínez-García, E., Jatsenko, T., Kivisaar, M., de Lorenzo, V., 2015. Freeing *Pseudomonas putida* kt 2440 of its proviral load strengthens endurance to environmental stresses. *Environmental Microbiology* 17 (1), 76–90.
- Mathee, K., Narasimhan, G., Valdes, C., Qiu, X., Matewish, J.M., Koehrsen, M., Rokas, A., Yandava, C.N., Engels, R., Zeng, E., et al., 2008. Dynamics of *Pseudomonas aeruginosa* genome evolution. *Proceedings of the National Academy of Sciences* 105 (8), 3100–3105.
- Mosquera-Rendón, J., Rada-Bravo, A.M., Cárdenas-Brito, S., Corredor, M., Restrepo-Pineda, E., Benítez-Páez, A., 2016. Pangenome-wide and molecular evolution analyses of the *Pseudomonas aeruginosa* species. *BMC Genomics* 17 (1), 45.
- Nanda, A.M., Thormann, K., Frunzke, J., 2015. Impact of spontaneous prophage induction on the fitness of bacterial populations and host-microbe interactions. *Journal of Bacteriology* 197 (3), 410–419.
- Nixon, G.M., Armstrong, D.S., Carzino, R., Carlin, J.B., Olinsky, A., Robertson, C.F., Grimwood, K., 2001. Clinical outcome after early *Pseudomonas aeruginosa* infection in cystic fibrosis. *The Journal of Pediatrics* 138 (5), 699–704.
- Oppenheim, A.B., Adhya, S.L., et al., 2007. A new look at bacteriophage λ genetic networks. *Journal of Bacteriology* 189 (2), 298–304.
- Payne, R.J., Jansen, V.A., 2001. Understanding bacteriophage therapy as a density-dependent kinetic process. *Journal of Theoretical Biology* 208 (1), 37–48.
- Payne, R.J.H., Jansen, V.A.A., 2003. Pharmacokinetic principles of bacteriophage therapy. *Clinical Pharmacokinetics* 42, 315–325.
- Price, K.E., Hampton, T.H., Gifford, A.H., Dolben, E.L., Hogan, D.A., Morrison, H.G., Sogin, M.L., O'Toole, G.A., 2013. Unique microbial communities persist in individual cystic fibrosis patients throughout a clinical exacerbation. *Microbiome* 1 (1), 27.
- Rakonjac, J., 2012. Filamentous Bacteriophages: Biology and Applications. *American Cancer Society*. <https://doi.org/10.1002/9780470015902.a0000777>. arXiv: <https://onlinelibrary.wiley.com/doi/pdf/10.1002/9780470015902.a0000777>. URL: <https://onlinelibrary.wiley.com/doi/abs/10.1002/9780470015902.a0000777>.
- Rapti, Z., Cáceres, C., 2016. Effects of intrinsic and extrinsic host mortality on disease spread. *Bulletin of Mathematical Biology* 78, 235–253.
- Rapti, Z., 2021. Temperate and chronic virus competition. University of Illinois at Urbana-Champaign. https://doi.org/10.13012/B2IDB-0705058_V1.
- Rokney, A., Kobiler, O., Amir, A., Court, D.L., Stavans, J., Adhya, S., Oppenheim, A.B., 2008. Host responses influence on the induction of lambda prophage. *Molecular Microbiology* 68 (1), 29–36.
- Roux, S., Hallam, S.J., Woyke, T., Sullivan, M.B., 2015. Viral dark matter and virus-host interactions resolved from publicly available microbial genomes. *Elife* 4, e08490.
- Schrader, H.S., Schrader, J.O., Walker, J.J., Wolf, T.A., Nickerson, K.W., Kokjohn, T.A., 1997. Bacteriophage infection and multiplication occur in *Pseudomonas aeruginosa* starved for 5 years. *Canadian Journal of Microbiology* 43 (12), 1157–1163.
- Shapiro, J.W., Williams, E.S., Turner, P.E., 2016. Evolution of parasitism and mutualism between filamentous phage m13 and *Escherichia coli*. *PeerJ* 4, e2060.
- Silpe, J.E., Bassler, B.L., 2018. A host-produced quorum-sensing autoinducer controls a phage lysis-lysogeny decision. *Cell*.
- Simmons, M., Drescher, K., Nadell, C.D., Bucci, V., 2017. Phage mobility is a core determinant of phage-bacteria coexistence in biofilms. *The ISME Journal* 12 (2), 531.
- Sinha, V., Goyal, A., Svenningsen, S.L., Semsey, S., Krishna, S., 2017. In silico evolution of lysis-lysogeny strategies reproduces observed lysogeny propensities in temperate bacteriophages. *Frontiers in Microbiology* 8, 1386.
- Spalding, C., Keen, E., Smith, D.J., Krachler, A.-M., Jabbari, S., 2018. Mathematical modelling of the antibiotic-induced morphological transition of *Pseudomonas aeruginosa*. *PLoS Computational Biology* 14, (2) e1006012.
- Spencer, D.H., Kas, A., Smith, E.E., Raymond, C.K., Sims, E.H., Hastings, M., Burns, J.L., Kaul, R., Olson, M.V., 2003. Whole-genome sequence variation among multiple isolates of *Pseudomonas aeruginosa*. *Journal of Bacteriology* 185 (4), 1316–1325.
- Stent, G.S., et al., 1963. Molecular biology of bacterial viruses., *Molecular biology of bacterial viruses.*
- St-Pierre, F., Endy, D., 2008. Determination of cell fate selection during phage lambda infection. *Proceedings of the National Academy of Sciences* 105 (52), 20705–20710.
- Stressmann, F.A., Rogers, G.B., Marsh, P., Lilley, A.K., Daniels, T.W., Carroll, M.P., Hoffman, L.R., Jones, G., Allen, C.E., Patel, N., Forbes, N., Forbes, B., Tuck, A., Bruce, K.D., 2011. Does bacterial density in cystic fibrosis sputum increase prior to pulmonary exacerbation? *Journal of Cystic Fibrosis* 10 (5), 357–365.
- Sulakvelidze, A., Alavidze, Z., Morris, J.G., 2001. Bacteriophage therapy. *Antimicrobial Agents and Chemotherapy* 45 (3), 649–659.
- Tabib-Salazar, A., Liu, B., Shadrin, A., Burchell, L., Wang, Z., Wang, Z., Goren, M.G., Yosef, I., Qimron, U., Severinov, K., et al., 2017. Full shut-off of *Escherichia coli* rna-polymerase by $\tau 7$ phage requires a small phage-encoded dna-binding protein. *Nucleic Acids Research* 45 (13), 7697–7707.
- Thingstad, T.F., Våge, S., Storesund, J.E., Sandaa, R.-A., Giske, J., 2014. A theoretical analysis of how strain-specific viruses can control microbial species diversity. *Proceedings of the National Academy of Sciences* 111 (21), 7813–7818.
- US Department of Health and Human Services, 2013. Antibiotic resistance threats in the united states, 2013, Centers for Disease Control and Prevention.
- Vidakovic, L., Singh, P.K., Hartmann, R., Nadell, C.D., Drescher, K., 2018. Dynamic biofilm architecture confers individual and collective mechanisms of viral protection. *Nature Microbiology* 3 (1), 26.
- Volkova, V.V., Lu, Z., Besser, T., Gröhn, Y.T., 2014. Modeling the infection dynamics of bacteriophages in enteric *Escherichia coli*: estimating the contribution of transduction to antimicrobial gene spread. *Applied and Environmental Microbiology* 80 (14), 4350–4362.
- Wahl, L.M., Betti, M.I., Dick, D.W., Pattenden, T., Puccini, A.J., 2019. Evolutionary stability of the lysis-lysogeny decision: Why be virulent? *Evolution* 73 (1), 92–98.
- Weinbauer, M.G., 2004. Ecology of prokaryotic viruses. *FEMS Microbiology Reviews* 28 (2), 127–181.
- Weitz, J.S., Dushoff, J., 2008. Alternative stable states in host-phage dynamics. *Theoretical Ecology* 1 (1), 13–19.
- Weitz, J.S., Li, G., Gulbudak, H., Cortez, M.H., Whitaker, R.J., 2019. Viral invasion fitness across a continuum from lysis to latency. *Virus Evolution* 5(1):vez006..
- Winstanley, C., Langille, M.G., Fothergill, J.L., Kukavica-Ibrulj, I., Paradis-Bleau, C., Sanschagrin, F., Thomson, N.R., Winsor, G.L., Quail, M.A., Lennard, N., et al., 2009. Newly introduced genomic prophage islands are critical determinants of in vivo competitiveness in the liverpool epidemic strain of *Pseudomonas aeruginosa*. *Genome Research* 19 (1), 12–23.
- You, L., Suthers, P.F., Yin, J., 2002. Effects of *Escherichia coli* physiology on growth of phage $\tau 7$ in vivo and in silico. *Journal of Bacteriology* 184 (7), 1888–1894.
- Yu, X., Xu, Y., Gu, Y., Zhu, Y., Liu, X., 2017. Characterization and genomic study of 'phikmv-like' phage paxyb1 infecting *Pseudomonas aeruginosa*. *Scientific Reports* 7 (1), 13068.
- Zwietering, M., Jongenburger, I., Rombouts, F., Van't Riet, K., 1990. Modeling of the bacterial growth curve. *Applied and Environmental Microbiology* 56 (6), 1875–1881.